



Tool Condition Monitoring in machining for the workpiece surface quality evaluation

Downloaded from: <https://research.chalmers.se>, 2024-06-30 16:40 UTC

Citation for the original published paper (version of record):

Del Prete, A., Nyborg, L., Franchi, R. et al (2024). Tool Condition Monitoring in machining for the workpiece surface quality evaluation. *Materials Research Proceedings*, 41: 2011-2020.
<http://dx.doi.org/10.21741/9781644903131-222>

N.B. When citing this work, cite the original published paper.

Tool Condition Monitoring in machining for the workpiece surface quality evaluation

DEL PRETE Antonio^{1,a}, NYBORG Lars^{2,b}, FRANCHI Rodolfo^{1,c*} and PRIMO Teresa^{1,d}

¹Via per Monteroni, Building "O", Ecotekne Campus, 73100 Lecce, Italy

²Chalmers University of Technology, 412 96 Gothenburg, Sweden

^aantonio.delprete@unisalento.it, ^blars.nyborg@chalmers.se, ^crodolfo.franchi@unisalento.it, ^dteresa.primo@unisalento.it

Keywords: Tool Condition Monitoring, Machining, Surface Quality

Abstract. Achieving high surface quality is crucial in manufacturing, impacting product functionality and appearance. Poor quality can lead to defects, friction, and safety risks. Cutting tools endure harsh conditions and wear over time, affecting surface quality and increasing costs. Monitoring tool condition is vital for efficiency, reducing cycle times and downtime. Industries like aerospace and automotive require tight quality control for meeting standards. Historically, manual inspections and scheduled changes were used, but advanced technology now allows more efficient tool condition monitoring. The paper outlines a tool condition monitoring approach using sensors and machine learning to predict and classify tool conditions and workpiece surface quality. It integrates acoustic emission, accelerometer, and thermal infrared camera sensors into a lathe machine. Various machine learning algorithms are trained and validated to accurately predict tool and surface conditions. The most effective model is identified and presented.

Introduction

The adoption of smart production in Industry 4.0 offers a range of tangible benefits, including cost reduction, improved operational efficiency, and enhanced product quality [1]. This approach enables the creation of flexible and adaptable production systems capable of responding in real-time to changing market demands [2]. Process monitoring through the use of sensors, data analytics, and machine learning algorithms allows for the timely detection and resolution of defects and issues, optimizing production [3].

Surface roughness in machining is influenced by various factors, including cutting speed, feed rate, depth of cut, and tool wear [4]. Sensors such as acoustic emission, accelerometers, and infrared devices are employed to monitor tool conditions and the quality of the machined surface, contributing to process optimization [5] [6].

Analysis of statistical characteristics of sensor signals enables assessment of tool health, with several studies exploring correlations between sensor data and tool wear [7] [8]. Machine learning techniques also represent a step forward in improving tool condition monitoring systems [9].

Timely detection of tool wear through sensor monitoring allows for prompt intervention, minimizing the impact on efficiency and quality of the machining process [10]. However, there remains a knowledge gap regarding the correlation between roughness, temperature, and tool wear based on signal characteristics [11]. Consistently with the context above described, this paper presents the development of a system for TCM implementing different kind of sensors for the quality process control. The set of sensors used for the scope consists of an accelerometer (Acc), an AE sensor and an infrared thermal camera (IRTC). Thus, the results of a preliminary experimental activity having as objective data acquisition for tool wear and surface quality modelling are here presented. Different cutting speed values were considered, under fixed feed

rate and depth of cut. In these conditions, flank wear V_b , surface roughness R_a and temperature T at the tool-chip interface were monitored at different time steps. The signals of the Acc and AE sensors were adequately windowed and filtered for the noise reduction, and a set of features were from them extracted. A Principal Component Analysis (PCA) was performed in order to reduce the problem dimensionality. Then, different regression Machine Learning models for V_b , R_a and T were developed and evaluated, highlighting the strong correlation between R_a , V_b and T . A practical case of the methodology utilization is presented, demonstrating the high potential of the methodology application in the specific turning process. Finally, the best performing model is presented.

Materials and methods

Fig.1 shows a schematic representation of the developed TCM methodology workflow; the followings phases were adequately considered:

Data Collection: Gathering of relevant data from the machining process, including information about tool condition and associated features such as vibration data, acoustic emissions, temperature, cutting forces, and machining parameters.

Data Preprocessing: Preparing and cleaning the data, involving handling missing values, noise reduction, and normalization.

Data Augmentation and Splitting: Creating new training examples by making various transformations or modifications to existing data; splitting of the dataset into training, validation, and testing sets for machine learning models setup.

Feature Selection: Performing feature selection to identify the most important features for the model.

Model Selection: Choosing appropriate machine learning algorithms or models for the specific problem.

Model Training: Training the selected machine learning models using the training dataset. Fine-tune hyperparameters through cross-validation on the validation set to optimize the model's performance.

Model Evaluation: Assessing the models' performance on the test dataset using appropriate evaluation metrics.

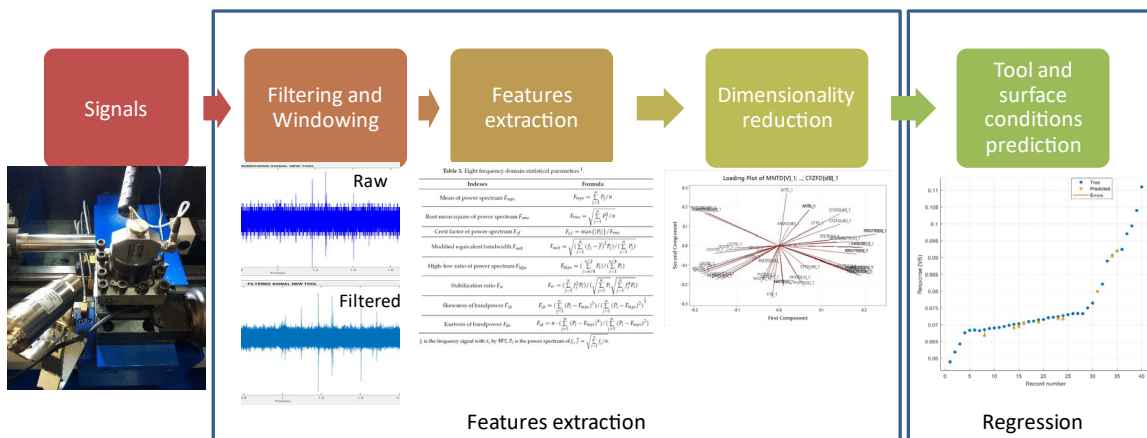


Fig.1. Adopted TCM methodology.

To gather relevant data from the machining process, machining turning tests were performed. The material under investigation is the S235jr steel, complying with the EN 10025-2 standard; Table 1 reports its chemical composition.

Table 1. Chemical composition of the S235JR steel [12].

Element	%weight
Carbon, C	0.17
Phosphorus, P	0.035
Silicon, Si	0.045
Manganese, Mn	1.4
Nitrogen, N	0.012
Copper, Cu	0.55

Machining tests were performed on bars having a diameter equal to 35 mm and an overhang equal to 100 mm. The adopted lathe machine is a SOGI M2C-450. The TCM methodology was carried out implementing on the lathe machine the following experimental setup:

- An accelerometer for vibration detection (8763b Kistler, Switzerland)
- An acoustic emission sensor (8152C Kistler, Switzerland)
- An infrared thermo-camera (Optris Xi 410).

The software Elsys Tranax 4.0 was used for the Acc and AE signals acquisition; for the thermal imaging, the software Optrix Pix Connect was used.

Fig. 2 reports the experimental setup.

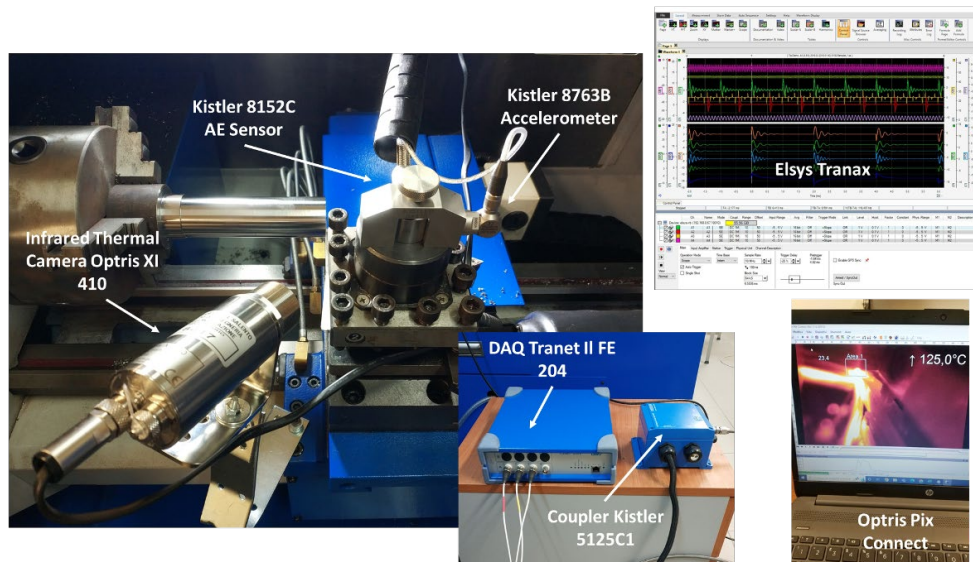


Fig.2. Experimental setup for turning.

As shown in the figure, the Acc and the AE sensors were fixed near the tool holder. The IRTC was mounted on a rigid bracket and placed, also, near the tool holder.

Thus, it was possible to keep the focus directly on the cutting zone following the movement of the tool during the entire process duration. Then, during the experimental tests, the signal acquired by IRTC indicated the thermal gradient into the cutting zone.

The IRTC emissivity was calibrated in the temperature range 25°C-250°C; method chosen by authors involved heating up by cutting to a known temperature, measured with use of noncontact thermometer, and then measuring the target temperature with the infrared camera. The next step was changing the emissivity until the temperature corresponds to that of the thermometer. Emissivity value determined this way would be use for all future measurements.

Further, for the tool wear measurements (complying with the ISO-3685 standard) and the roughness Ra evaluations (complying with the ISO-1997 standard) the following experimental equipment were adopted:

- Dinolite AM7915MZTL Microscope;
- Mahr MarSurf PS10 SET Portable digital roughness tester.

The experimental campaign was carried out under dry conditions; the considered time steps for the responses of interests and the signals acquisitions have been set on 1 minute.

The experiments were performed at the following cutting parameters:

- Cutting speed, $v_c=65\text{m/min} - 90\text{m/min} - 115\text{m/min}$;
- Feed rate, $f=0.075\text{mm/rev}$;
- Dept of cut, $p=0.5\text{mm}$.

The cutting tool used in the experimental activity is a Mitsubishi CCMT060204 M grade; the cutting parameters were selected based on the manufacturer's recommendations.

As output, the followings responses have been considered:

1. Roughness, R_a ;
2. Tool wear V_b ;
3. Temperature T .

The Acc and AE signals were acquired with a 2.5 MHz sample rate; the signals processing and analysis was performed in Matlab 2021 environment. To remove the noise due to the different occurrences not directly related with the process, the Acc and AE signals were adequately filtered, and a Hamming window was them applied to the signals to mitigate the adverse effects of impulse response truncation. In particular, the Acc signals (in x, y and z directions) were filtered with a low pass FIR filter, with a 250 kHz cut frequency while the AE signals were filtered with a high pass FIR filter, with a 10 kHz threshold frequency. Finally, the Power Spectrum Density was calculated to analyse the signals in the frequency domain. To verify the repeatability of the process, three replicas were carried out. Fig.3 shows, for the test with $v_c=90\text{m/min}$, an example of AE signal Power Spectrum related to all the replicas; it is possible to observe that the process is reasonably repeatable.

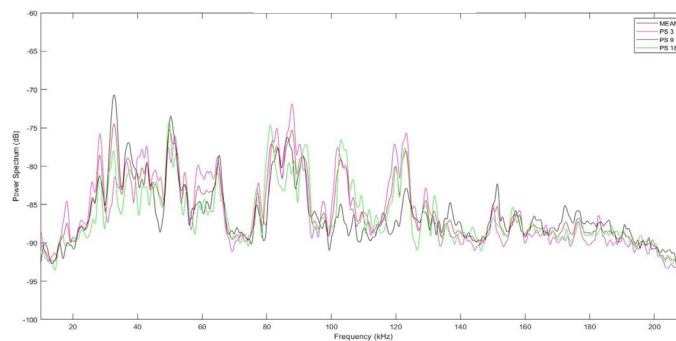


Fig.3. AE signal Power Spectrum.

In the Feature extraction phase, a set of 40 features in the Time and Frequency domains were extracted from the Acc and AE sensors signals. The considered features in the Time Domain are listed as follows: Mean, Standard Deviation, Root Mean Square (RMS), Peak to Peak, Peak to Valley, Crest Factor and Kurtosis. The considered features in the Frequency Domain are listed as follows: Mean, Root Mean Square (RMS) and Crest Factor.

To reduce the problem complexity and to manage with less dimensions, a Principal Components Analysis was performed (Dimensionality reduction phase); the 40 features were reduced to 12 considering the scores S1-S12, without a loss of information content (there was still a 96% explained variance with only 12 features).

T, V_b and R_a were acquired during the experimental tests; Fig.4 shows how the data were operationally collected.

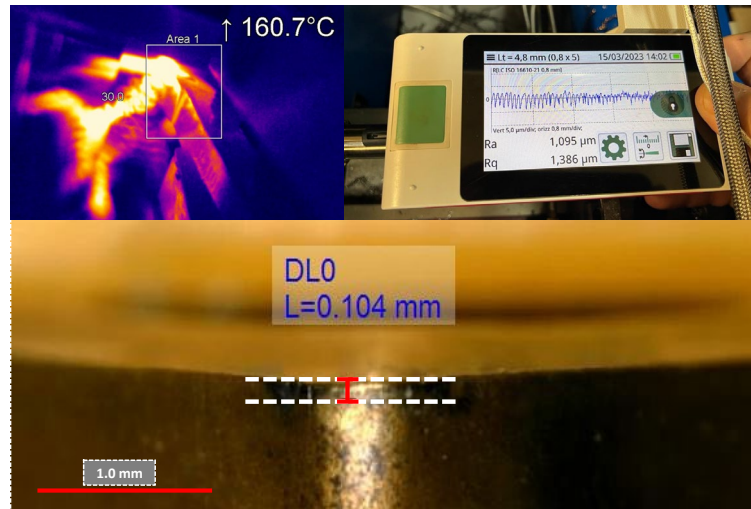


Fig.4. Data acquisition operative modes.

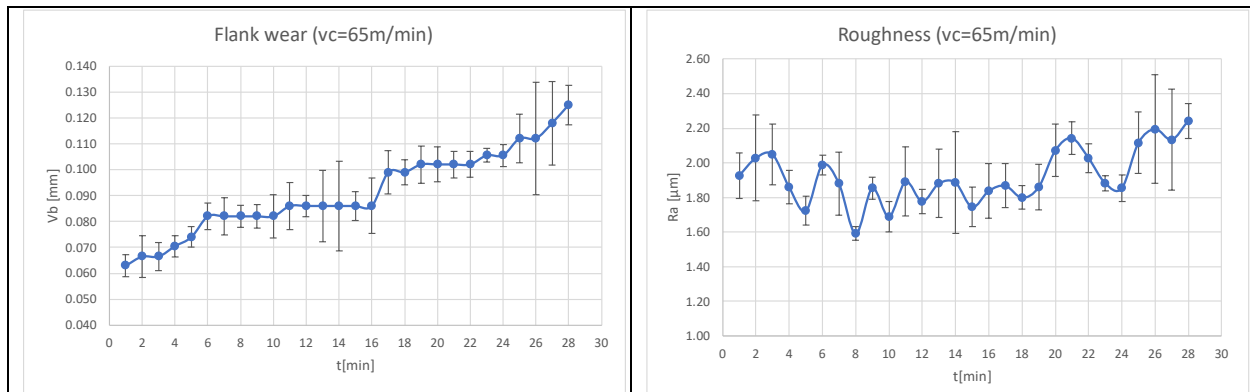
Finally, in the tool wear, roughness, and temperature conditions prediction phase, the followings different algorithms were trained and tested:

1. Decision Tree, with two different values of Minimum Life Size: DT-4, DT-12;
2. Artificial Neural Network, with two different values of the First Layer Size: ANN-10, ANN-25;
3. Support Vector Machine, with two different kernel functions: SVM-Q, SVM-C;
4. Gaussian Process Regression, with two different kernel functions: GPR-RQ, GPR-M5/2;
5. Gaussian Process Regression, with bayesian optimization: GPR-BO.

The models learning phase (training and validation) was performed using the 60% of the overall data for the training and the 20% for the validation. The resting 20% of the data was used for the testing phase. For the development of the models, the Matlab 2021 environment was used.

Results

In Fig.5 are represented the trends of Vb and roughness, acquired during the experimental activity (the error bars are reported). As can be seen from the graphs, the trends of these responses are consistent with the behaviors widely described in the literature [13].



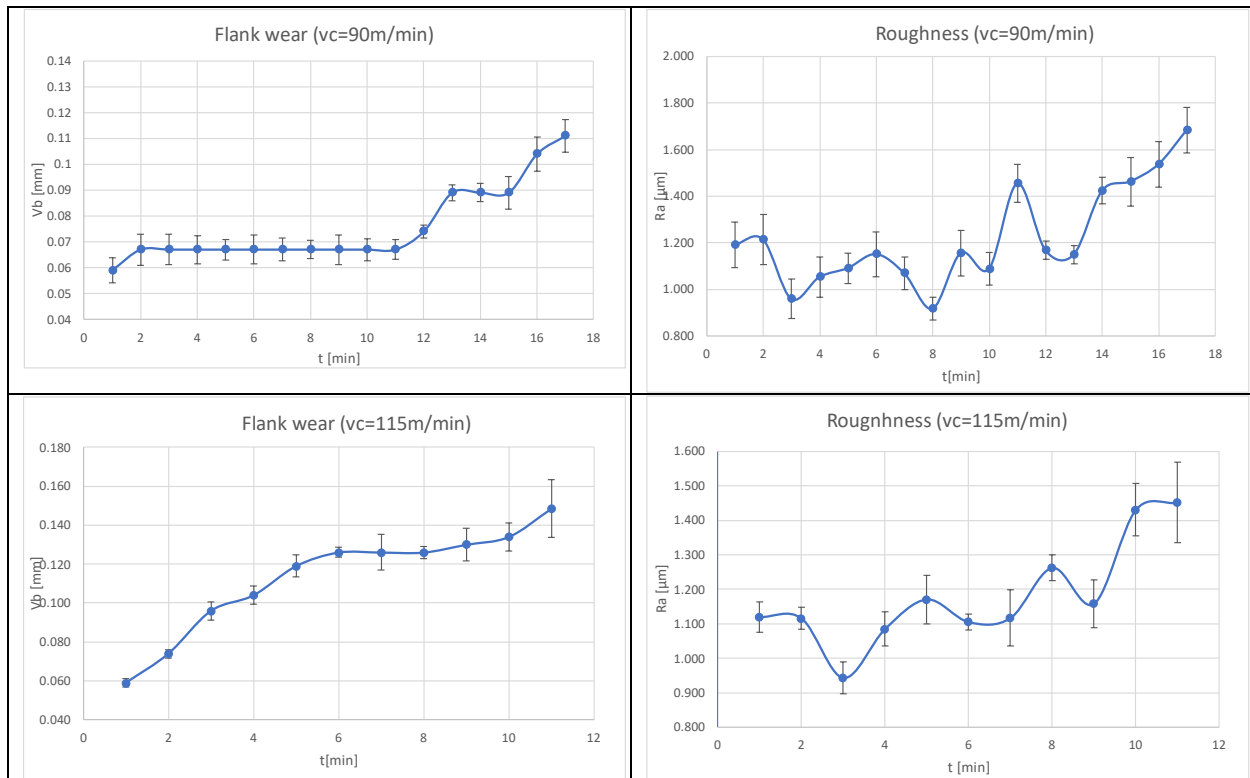


Fig.5. *Vb and roughness experimental trends.*

Because the original dataset was sparse, the Makima interpolation technique was utilized to create new data points between existing ones, to generate a more extensive dataset. Therefore, the time steps were augmented obtaining data every 30 seconds, and 11 levels were added to the cutting speed values range (65m/min to 115m/min). This increased from 56 to 390 observations.

All data, including temperature, were used to train and validate the responses regression models as functions of the time t and the S1-S12 scores, obtained from the application of the PCA to the 40 features extracted from the Acc and AE signals. Then, the following models were developed and tested:

- $VB=VB(t,S1,S2,S3,S4,S5,S6,S7,S8,S9,S10,S11,S12)$;
- $Ra=Ra(t,S1,S2,S3,S4,S5,S6,S7,S8,S9,S10,S11,S12)$;
- $T=T(t,S1,S2,S3,S4,S5,S6,S7,S8,S9,S10,S11,S12)$.

Fig.6 shows the results obtained about the performances of Vb , Ra and T models. For all of them, RMSE and R-Squared values obtained both during the models' validation and testing phases, are presented. The RMSE index is related with the prediction error: the lower this index, the higher the model accuracy. On the other hand, the R-Squared index is function of the portion of the total variability explained by the model: the closer this index is to 1, the more accurate the model is.

Regarding the Vb regression, GPR models exhibits the lowest RMSE values and the highest R-Squared values; GPR with Bayesian optimization (GPR-BO) can be considered the most performing algorithm.

About the Ra regression, GPR models, particularly the GPR-BO, still excel in terms of RMSE and R-Squared.

Finally, about the T regression, there is a clear distinction between the performance offered by the GPR algorithms and others such as DT and ANN.

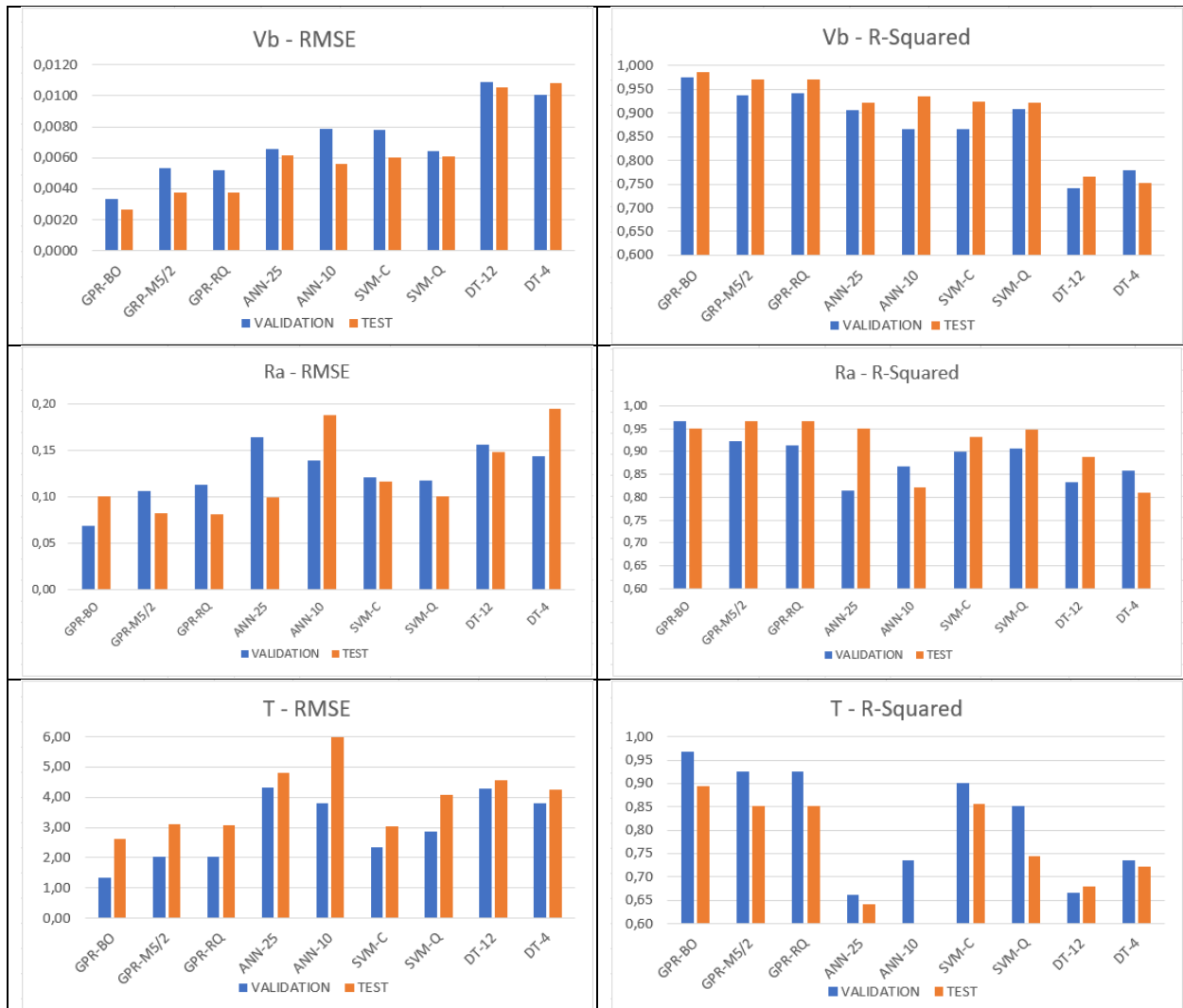


Fig.6. Vb, Ra and T models performances: RMSE and R-Squared values.

Fig.7 shows the responses vs record number and the predicted vs true plots related to the Vb, Ra and T GPR-BO models.

The "responses vs record number" plot shows how the responses in the dataset change concerning the record number or index of the data: the plot shows how the response variable changes over time.

The "true vs predicted" plot is a visualization used to evaluate the performance of a predictive model, especially in regression or estimation tasks. It compares the actual (true) values of the target variable against the predicted values generated by the model.

As for the trends of Vb over time, ordered by increasing cutting speeds, it can be observed that at high speeds the curves are steeper and contain fewer observations. The difference between actual observations, in blue, and predicted observations, in orange, is minimal. About the Vb true vs predicted response plot, it shows how the observations are densely distributed around the line of perfect prediction. For Vb values below 0.1mm, the prediction is extremely accurate; with the evolution of the process, the contribution of uncontrollable phenomena is more marked, then the model predictions are less accurate. This occurrence is more evident in the Fig.8 where the experimental Standard Deviation versus Vb are linked with the evidence in the True vs Predicted plot; as can be seen, the Standard Deviation increasing with the Vb (and then, with the time), probably also generating the spread of the True vs Predicted plot after a Vb of 0.1 mm.

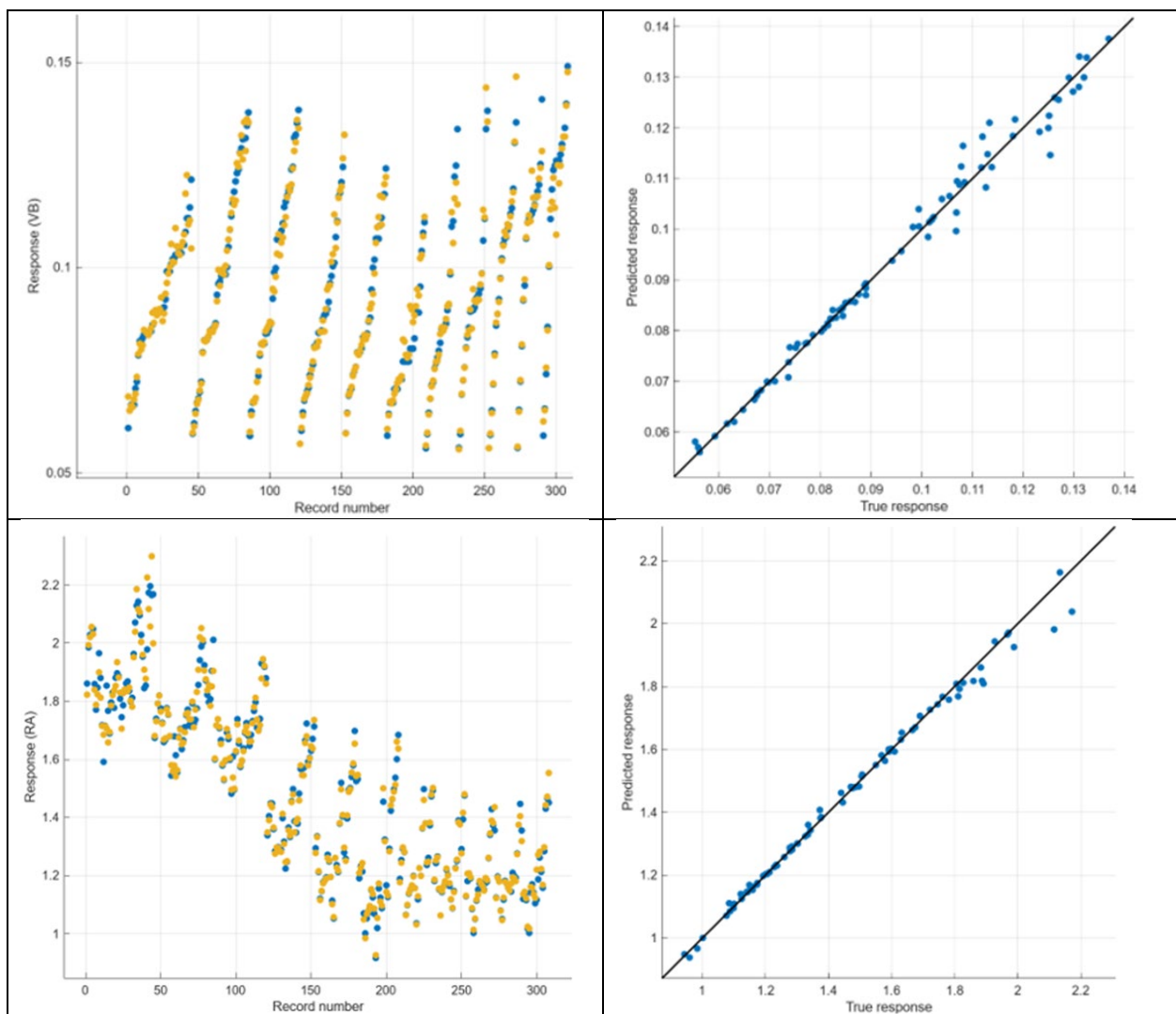
The Ra plot over time shows the tendency of the response to decrease as the cutting speed increases. From each the individual trends, after a running-in phase, Ra stabilizes and then increases as a announce of process drift.

From the true vs predicted plot it is immediate to observe the high predictive capacity of the Ra GPR-BO model, in fact almost all the 390 observations of the dataset lie on the perfect prediction line.

Finally, from the observation of the response vs record number and true vs predicted plots, even for T the GPR_BO model demonstrates to provide a high degree of accuracy.

Additionally, when examining plot response and record numbers, a discernible almost quadratic trend emerges in the relationship between T and cutting speed. The temperature rises with the increase in cutting speed until reaching a specific threshold, beyond which it begins to decrease.

This pattern is explicable by the heightened heat dissipation resulting from the higher Material Removal Rate (MRR) at elevated cutting speeds.



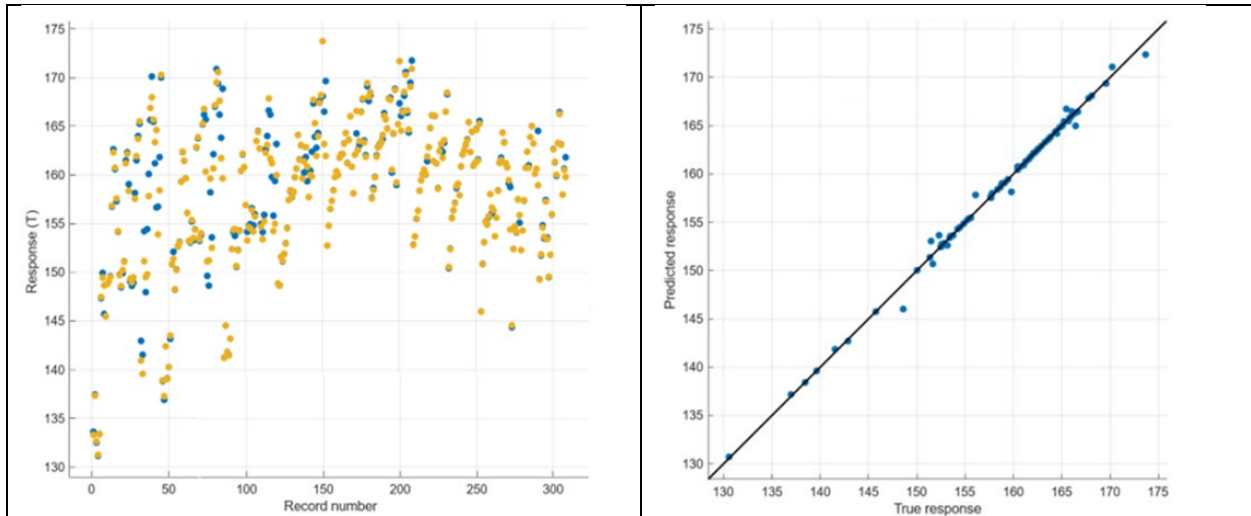


Fig.7. V_b , R_a and T models performances: responses vs record number plots (actual observations, in blue, predicted observations, in orange), predicted vs true response plots.

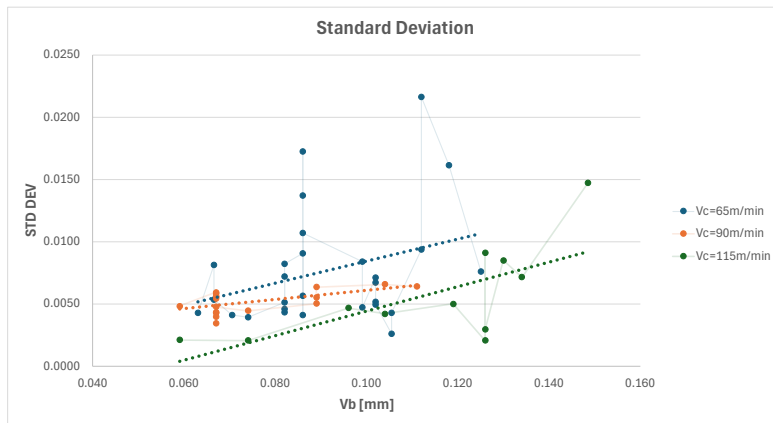


Fig.8. Standard Deviation vs V_b .

Conclusions and future developments.

This study evaluates the performance of artificial intelligence-based approaches for estimating roughness, tool wear and temperature at the tool/chip interface during turning of S235jr alloy steel. Different algorithms were trained to estimate the roughness, tool wear and temperature values in the process at several cutting speeds. The proposed models are developed on a dataset of 390 data points (60% of which are used in the training phase, 20% in the validation phase and the remaining 20% in the testing phase). The reported results show the feasibility of the GPR-BO models for estimating roughness, tool wear and temperature with high accuracy (RMSE and R-Squared were evaluated). The estimated values are in good agreement with the performed experiments and with the results reported in literature. The obtained results demonstrate the effectiveness of the Tool and Surface Conditions Monitoring based on previous training dataset in the reduction of the experimental work and resources. As future development, the authors will extend the experimental activity considering tests at different feed rate and depth of cut. Moreover, the developed models will be integrated in a process automation able of near real time anomaly detection.

In addition, the authors will develop a process automation integrating sensors, acquisition devices, analysis software, developed models and that will be able to perform anomaly detection in near real time.

References

- [1] Çelik, Y.H., Kilickap, E. & Güney, M. Investigation of cutting parameters affecting on tool wear and surface roughness in dry turning of Ti-6Al-4V using CVD and PVD coated tools. *J Braz. Soc. Mech. Sci. Eng.* 39, 2085–2093 (2017). <https://doi.org/10.1007/s40430-016-0607-6>
- [2] Saini, S., Ahuja, I.S. & Sharma, V.S. Influence of cutting parameters on tool wear and surface roughness in hard turning of AISI H11 tool steel using ceramic tools. *Int. J. Precis. Eng. Manuf.* 13, 1295–1302 (2012). <https://doi.org/10.1007/s12541-012-0172-6>
- [3] H.K. Tönshoff, I. Inasaki, *Sensors in Manufacturing, Volume 1*, 2001, Wiley-VCH Verlag GmbH. <https://doi.org/10.1002/3527600027>
- [4] M. S. H. Bhuiyan, I. A. Choudhury, Y. Nukman, Tool Condition Monitoring using Acoustic Emission and Vibration Signature in Turning, *Proceedings of the World Congress on Engineering 2012 Vol III WCE 2012, July 4 - 6, 2012, London, U.K.*
- [5] J. Ratava, M. Lohtander, J. Varis, Tool condition monitoring in interrupted cutting with acceleration sensors, *Robotics and Computer-Integrated Manufacturing, Volume 47*, 2017, Pages 70-75, ISSN 0736-5845, <https://doi.org/10.1016/j.rcim.2016.11.008>
- [6] B. S. Prasad, K. A. Prabha, P.V.S. Ganesh Kumar, Condition monitoring of turning process using infrared thermography technique – An experimental approach, *Infrared Physics & Technology, Volume 81*, 2017, Pages 137-147, ISSN 1350-4495. <https://doi.org/10.1016/j.infrared.2016.12.023>
- [7] K. Jemielniak, P.J. Arrazola, Application of AE and cutting force signals in tool condition monitoring in micro-milling, *CIRP Journal of Manufacturing Science and Technology, Volume 1, Issue 2*, 2008, Pages 97-102, ISSN 1755-5817, <https://doi.org/10.1016/j.cirpj.2008.09.007>
- [8] G. Serin & B. Sener & A. M. Ozbayoglu & H. O. Unver, Review of tool condition monitoring in machining and opportunities for deep learning, *The International Journal of Advanced Manufacturing Technology* (2020) 109:953–974. <https://doi.org/10.1007/s00170-020-05449-w>
- [9] Krzysztof Jemielniak & Tomasz Urbański & Joanna Kossakowska & Sebastian Bombiński, Tool condition monitoring based on numerous signal features, *Int J Adv Manuf Technol* (2012) 59:73–81. <https://doi.org/10.1007/s00170-011-3504-2>
- [10] Mustafa Kuntoglu, Hacı Saglam, Investigation of signal behaviors for sensor fusion with tool condition monitoring system in turning, *Measurement Volume 173*, March 2021, 108582. <https://doi.org/10.1016/j.measurement.2020.108582>
- [11] Mustafa Kuntoglu, Abdullah Aslan, Hacı Saglam, Danil Yurievich Pimenov, Khaled Giasin and Tadeusz Mikolajczyk, Optimization and Analysis of Surface Roughness, Flank Wear and 5 Different Sensorial Data via Tool Condition Monitoring System in Turning of AISI 5140, 2020 *Sensors*. <https://doi.org/10.3390/s20164377>
- [12] Pauline Ong, Woon Kiow Lee & Raymond Jit Hoo Lau, Tool condition monitoring in CNC end milling using wavelet neural network based on machine vision, *The International Journal of Advanced Manufacturing Technology* (2019) 104:1369–1379. <https://doi.org/10.1007/s00170-019-04020-6>
- [13] P.G. Benardos, G.-C. Vosniakos, Predicting surface roughness in machining: a review, *International Journal of Machine Tools and Manufacture, Volume 43, Issue 8*, 2003, Pages 833-844, ISSN 0890-6955. [https://doi.org/10.1016/S0890-6955\(03\)00059-2](https://doi.org/10.1016/S0890-6955(03)00059-2)